AD-A113 647 ARMY ARMAMENT RESEARCH AND DEVELOPMENT COMMAND ABERD--ETC F/G 4/1
WATER VAPOR: ITS STRUCTURE AND ELECTROMAGNETIC ABSORPTION.(U)
MAR 82 H R CARLON

UNCLASSIFIED ARCSL-SP-81025 NL

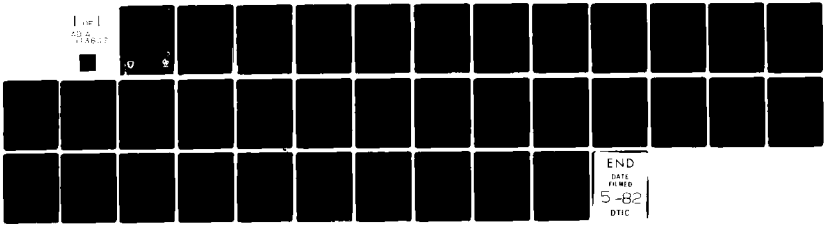

END
DATE FILMED
5-82
DTIC

AD

CHEMICAL SYSTEMS LABORATORY SPECIAL PUBLICATION

ARCSL-SP-81025

WATER VAPOR: ITS STRUCTURE AND ELECTROMAGNETIC ABSORPTION

by

Hugh R. Carlon

Research Division

March 1982

US ARMY ARMAMENT RESEARCH AND DEVELOPMENT COMMAND
Chemical Systems Laboratory
Aberdeen Proving Ground, Maryland 21010

Disclaimer

The findings in this report are not to be construed as an official Department of the Army position unless so designated by other authorized documents.

Disposition

Destroy this report when it is no longer needed. Do not return it to the originator.

UNCLASSIFIED

SECURITY CLASSIFICATION OF THIS PAGE (When Data Entered)

REPORT DOCUMENTATION PAGE		READ INSTRUCTIONS BEFORE COMPLETING FORM
1. REPORT NUMBER ARCSL-SP-81025	2. GOVT ACCESSION NO.	3. RECIPIENT'S CATALOG NUMBER
4. TITLE (and Subtitle) WATER VAPOR: ITS STRUCTURE AND ELECTROMAGNETIC ABSORPTION		5. TYPE OF REPORT & PERIOD COVERED Special Publication January–September 1981 6. PERFORMING ORG. REPORT NUMBER
7. AUTHOR(s) Hugh R. Carlon		8. CONTRACT OR GRANT NUMBER(s)
9. PERFORMING ORGANIZATION NAME AND ADDRESS Commander/Director, Chemical Systems Laboratory ATTN: DRDAR-CLB Aberdeen Proving Ground, Maryland 21010		10. PROGRAM ELEMENT, PROJECT, TASK AREA & WORK UNIT NUMBERS 1L161101A91A
11. CONTROLLING OFFICE NAME AND ADDRESS Commander/Director, Chemical Systems Laboratory ATTN: DRDAR-CLJ-R Aberdeen Proving Ground, Maryland 21010		12. REPORT DATE March 1982 13. NUMBER OF PAGES 40
14. MONITORING AGENCY NAME & ADDRESS(if different from Controlling Office)		15. SECURITY CLASS. (of this report) UNCLASSIFIED 15a. DECLASSIFICATION/DOWNGRADING SCHEDULE NA

16. DISTRIBUTION STATEMENT (of this Report)

Approved for public release; distribution unlimited.

17. DISTRIBUTION STATEMENT (of the abstract entered in Block 20, if different from Report)

18. SUPPLEMENTARY NOTES

19. KEY WORDS (Continue on reverse side if necessary and identify by block number)

Infrared	Water clusters	Atmospheric propagation
Absorption	Clusters, water	Electromagnetic radiation
Water	Clusters, molecular	Continuum absorption
Water vapor	Atmosphere	

(Continued on reverse side)

20. ABSTRACT (Continue on reverse side if necessary and identify by block number)

Research has shown that traditional theories of the structure of vapors are imprecise when applied to strongly hydrogen-bonded substances like water. Presented here are the main points of a new theory, with major emphasis on physical descriptions of the populations, sizes, and size distributions of neutral molecular cluster species in water vapor and moist air that interact with electromagnetic radiation in the atmosphere. From this theory, models are developed that

(Continued on reverse side)

DD FORM 1 JAN 73 1473 EDITION OF 1 NOV 65 IS OBSOLETE

UNCLASSIFIED

SECURITY CLASSIFICATION OF THIS PAGE (When Data Entered)

19. KEYWORDS (Contd.)

Cloud microphysics
Ions
Vapor electrical conductivity
Mass spectrometry

20. ABSTRACT (Contd.)

describe the infrared continuum absorption of atmospheric water vapor almost precisely, and extend this modeling to a wide range of temperatures and humidities. Because the new equations equations are based in fundamental physics, modeling in wavelength regions other than the infrared, e.g., the millimeter- and microwave-regions should be possible if investigators can compute and experimentally verify absorption attributable to modes of the neutral clusters that are effective in the absorption at these wavelengths. It is suggested that the new equations be incorporated into existing atmospheric transmission models.

PREFACE

The work described in this report was authorized under Project 1L161101A91A, In-House Laboratory Independent Research. This work was started in January 1981 and completed in September 1981.

CONTENTS

		Page
1.	INTRODUCTION	7
2.	THEORY	8
2.1	General	8
2.2	Data Interpretation from the New Theory	14
3.	THE INFRARED CONTINUUM ABSORPTION	16
4.	CONCLUSIONS	22
	LITERATURE CITED	25
	APPENDIX, Microphysics of Clouds and Nucleation Theory	29
	DISTRIBUTION LIST	37

WATER VAPOR: ITS STRUCTURE AND ELECTROMAGNETIC ABSORPTION

1. INTRODUCTION

Anomalous infrared (IR) absorption by atmospheric water vapor has been studied by the author[1-14] and by other workers[15-19] for several decades. In attributing this absorption to molecular clusters in water vapor, I have attempted always to interpret my data using traditional models of cloud physics, nucleation theory, and the kinetic theory of gases and liquids. During the past year, the cumulative correlation of data obtained from IR absorption measurements, mass spectra, electrical conductivity measurements of moist air, and thermodynamic and cluster models have indicated that the traditional models are imprecise when applied to strongly hydrogen-bonded substances like water. J. G. Wilson[20] suggested that the classical Thomson equation[21,22] and the model for droplet nucleation are ". . .clearly incomplete when, as for water, strongly polar molecules form an oriented surface layer..." Only relatively recently have detailed treatments of hydrogen bonding effects been undertaken,[23,6] even though Thomson, C. T. R. Wilson,[21,22] and other workers who formulated the basic concepts that have envolved into today's cloud microphysical, vapor cluster, and nucleation theories did so with absolutely no knowledge of hydrogen bonding.

My investigations to test the hypothesis that the IR continum absorption of water vapor results from liquid-like, hydrogen-bonded clusters of water molecules (monomers) in the vapor or in moist air have led to an apparent confirmation of the hypothesis, and to quantification of populations of neutral water clusters necessary to account for phenomena observed by IR and other techniques.

The purpose of this paper is to present the main points of a new theory that has evolved from my work, with major emphasis on physical descriptions of the populations, sizes, and size distributions of the neutral cluster species that interact with electromagnetic radiation in the atmosphere. Supporting measurements are described in the literature.[24-27] Because these physical descriptions now are available, it is possible to extend an analysis of the electromagnetic absorption and emission of vapor-phase neutral clusters beyond the confines of the IR continum absorption wavelength region and into, e.g., the millimeter-wave and microwave regions where related spectral effects also have been observed.[5,6] Since these spectral effects presumably also are due to the neutral water cluster distributions in moist or saturated air, a knowledge of the cluster species and their distributions should enable spectroscopists working in the millimeter-wave and microwave regions to predictively model absorption/emission by these water species in those wavelength regions.

The approach taken in this paper is to summarize background information and new theory with appropriate literature references for the interested reader. IR data, however, are discussed in considerable detail, and interpretations are supported by discussions of the theory. Because of the great sensitivity of cluster populations and size distributions to temperature and humidity as they are now understood, earlier estimates of these parameters from IR and other data must, in effect, be discarded. Values based on experimental data of many kinds that were only recently obtained are given here. These values, from their equations, should be considered for use in subsequent work since only in this way can users become familiar with the extent of agreement between theory and their own observations.

2. THEORY

2.1 General.

The new theory incorporates several elements that are decidely at odds with much of the present thinking on the nature of water vapor. These elements are first presented in general terms and later defended by presentations of the experimental evidence.

Water vapor and moist air contain enoumous populations of electrically neutral molecular clusters which are present in peaked statistical size distributions with typical mean sizes, c_u, of 10-30 or more water molecules (monomers) per cluster.[12-14] These neutral water clusters are formed by *evaporation* (distillation) of bulk liquid water, water solutions, or droplets. Only when liquid water is present in the system are the equilibria described in this paper achieved. When liquid water is completely removed from the system, the neutral cluster populations decay with half-life times on the order of 15 minutes to an hour or more,[25] and thus the history of the sample becomes important in determining, for instance, its IR spectral properties. Intermolecular and rotational modes of these neutral cluster distributions account for much (probably most) of the IR continuum absorption of water vapor and can precisely explain the amplitude and wavelength dependencies of this absorption, as will be shown later, although direct calculations of the absorption can be extremely complex because of the complexity of the variables. The neutral clusters dissociate to an extremely small extent at any instant of time[13,14,25,26] to yield ions by reactions that might be represented, e.g., by:

$$(H_2O)_{c+d+1} \longrightarrow H^+(H_2O)_c + OH^-(H_2O)_d \qquad (1)$$

or

$$HX(H_2O)_c \longrightarrow H^+(H_2O)_c + X^- \qquad (2)$$

where X^- could be a negative ion or an electron. The energetics of these reactions, of course, decidedly favor the reverse direction as indicated by my earlier discussion of expected cluster and ion mechanisms.[10] But subsequent experiments with corona discharges,[12] wherein it was deliberately attempted to enhance neutral cluster formation, produced no conclusive evidence of this. Instead, all data indicated that the ions came from the dissociation of neutral clusters already present in the vapor. This dissociation can be enhanced by using an ionization source, for example, a β-emitter.[12] In fact, radioactive disintegration is the source of much ionization in tropospheric moist air.[28] Thus the dissociation of the neutral clusters can be monitored by mass spectrometry of β-irradiated water vapor.[24-26] The electrical conductivity measurements of water vapor or moist air also involve the mobilities of the dissociative ions of the neutral clusters. Hence, these mobilities also are a measure of the cluster size (c), because larger clusters (as ions) move more slowly in an electrical field. Measurements recently made[29] involving these mobilities have shown that it is very likely that the most common dissociative reaction for neutral clusters, whether in normal moist air or for enhanced dissociation due to a β-emitter, simply is:

$$(H_2O)_{c+1} \xrightarrow{(\beta)} H^+(H_2O)_c + OH^- \qquad (3)$$

Thus the ion pairs formed by dissociation are greatly mismatched in size and mass.

Actual mass spectra[10,12] for β-irradiated moist air seem to bear out this hypothesis. For example, figure 1 shows the beautiful, near-Gaussian dissociative ion distributions for species $H^+(H_2O)_c$ from Eq 3 for several partial pressures resulting in the saturation ratios "s" (= %RH/100) shown, at 100°C. The number of monomers per cluster, "c," is shown on the abscissa and in Eq 3. Infrared measurements show that, if the neutral clusters producing the ions of size c in figure 1 are taken as having c + 1 size, virtually perfect agreement is obtained between computed spectra and the IR continuum absorption spectrum. But the existence of the neutral clusters is essential to account for the observed IR absorption because the population of ions is far too small to do so, as will be shown. Mass spectral measurements of the negative ions are planned. Note the higher-than-expected "spike" at c = 21 in the upper spectrum of figure 1. This corresponds to the population of neutral cluster having the favored low-energy configuration of a central monomer surrounded by a symmetrical pentagonal dodecahedron[23] which begins to approach a spherical shape. Such spikes always are observed in these spectra immediately to the left of a lower-than-expected population, e.g., c = 22 in the upper spectrum of figure 1. This allows the interpretation that the neutral clusters, except for very small open-chained ones, always have configurations such that one or more favored geometric solid-like structures are chained together or have tails of OH^- groups, or longer chains, attached to a hydrogen atom imbedded in the cluster cage matrix. Thus c = 21 is more populous because it corresponds to an OH^--depleted population added to the expected c = 21 cagelike population already present. This is exactly the sense of Eq 3.

Further defense of this interpretation of mass spectra is as follows. The technique of studying vapor-phase equilibria by the dynamic method of rapidly cooling gases to "freeze" the equilibrium,[30] that is, to prevent the shift of equilibrium, has been accepted in physical chemistry since at least as early as 1910 when Koref[31] reported its use to obtain very precise equilibrium constants for carbon disulfide. Precisely this kind of "freezing" takes place when a water vapor sample is subjected to rapid expansion and cooling from near-atmospheric pressure through a tiny orifice and into the high vacuum typical of mass spectrometers.[10] But it has been argued that mass spectra of water clusters, although they might contain related information, cannot be taken as direct representations of cluster ion distributions in moist air samples from which they are obtained,[32-33] primarily because the stresses of rapid expansion and extreme cooling (freezing) distort the resulting distributions that are observed. Certainly, it would be difficult to rationalize mass spectra obtained for typical moist air samples if it were assumed that they must form by the mechanism of monomer collision according to classical kinetic theory of gases and were then ionized by a radiation source in the mass spectrometer. The hydration of ions to form heterogeneous clusters that can be accurately studied by mass spectrometry is well documented,[34] but the situation is much less clear for plain water vapor where it must be assumed by kineticists that water monomers first are ionized and then hydrated to produce the observed mass (size) spectra. Indeed, a much simpler evaporative mechanism to explain the cluster distributions in the vapor, and their resulting mass spectra, can be shown to produce excellent agreement between theory and experiment.

Thus the dissociative ion cluster mass spectra of figure 1 can be argued to be nearly identical to the size spectra of the neutral cluster populations that produced them. If Eq 3 were correct, the spectra of figure 1 would be precisely those of the neutral clusters if the abscissa were relabeled (c + 1) instead of (c). This would explain the excellent agreement between the dissociative ion mass spectra and, for example, IR absorption trends with temperature and humidity.[10,12]

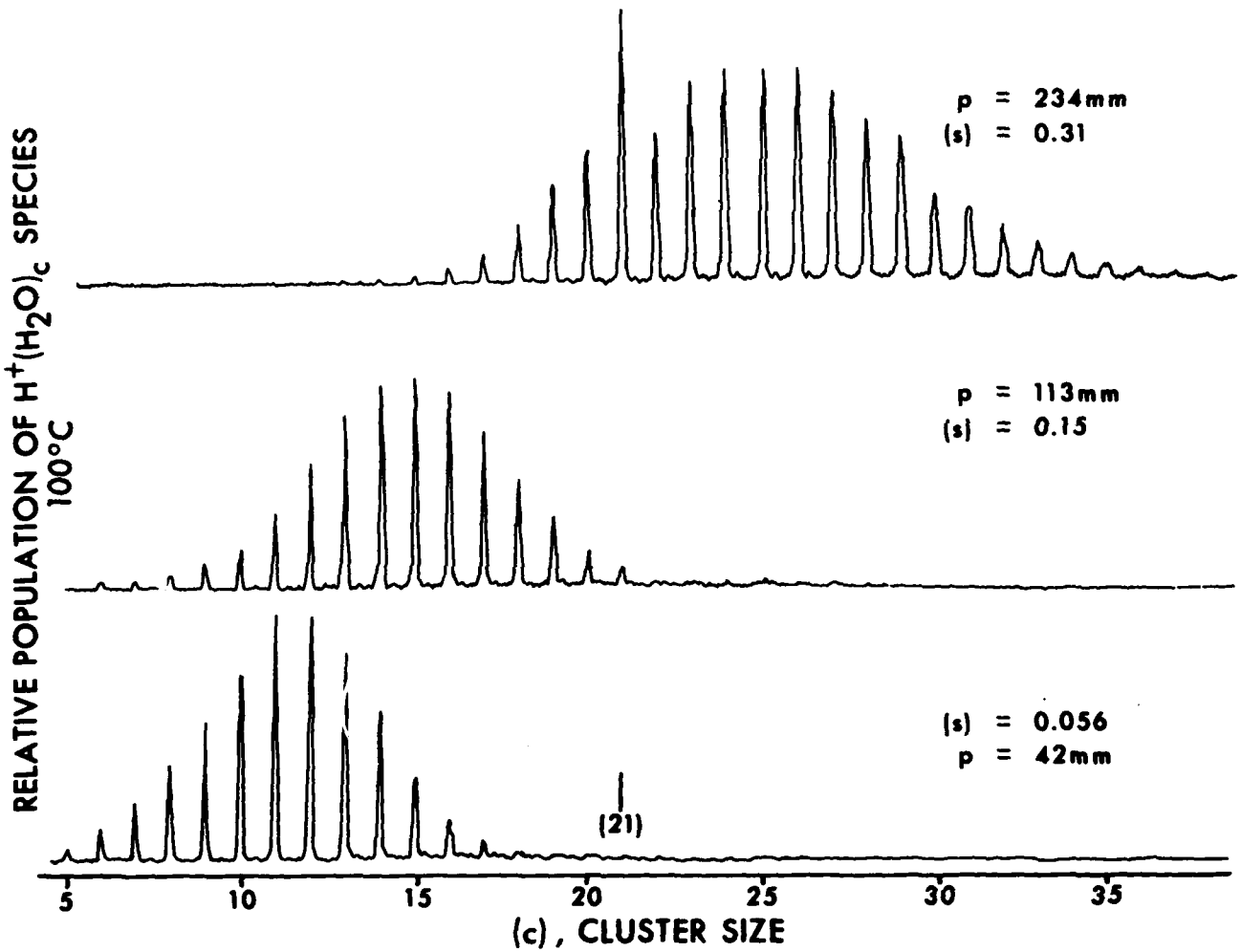

Figure 1. Mass Spectra of β-Irradiated Moist Air at Partial Water Vapor Pressures, p, mm Hg (Torr) and Saturation Ratios, s = %RH/100, Shown

All spectra are for 100°C, showing relative populations of $H^+(H_2O)_c$ species (Eq 3).

From Eq 3, the dissociative equilibrium product of the neutral clusters can be written:

$$K = \frac{{}^{a}H^{+}(H_2O)_c \cdot {}^{a}OH^{-}}{{}^{a}(H_2O)_{c+1}} \tag{4}$$

where a is the molar concentration of any species. For water, either in the liquid or the vapor phase, the magnitude of the denominator in Eq 4 remains almost constant because of the small extent to which water dissociates compared to other liquids or solutions. Thus the so-called ion product, K_w, of water is used instead as the equilibrium dissociation constant, and it is widely tabulated. This product is also capable of being used in equations to model the temperature dependence of the IR continuum absorption.[8,9,13] The ion product is:

$$K_w = {}^{a}H^{+}(H_2O)_c \cdot {}^{a}OH^{-} \tag{5}$$

If we now designate the total population or number of neutral water clusters of all sizes in 1 cc of water vapor or moist air as N_{cc}, and the number of dissociative ions of these clusters per cc at any instant as I_{cc}, it is easy to see that:

$$I_{cc} = (k)2\sqrt{K_w}(N_{cc}) \tag{6}$$

where k is a normalizing constant and "2" in Eq 6 indicates that ion pairs are formed according to Eq 3. But when actual measurement data are used to evaluate k in Eq 6, it is found that k ~0.5 or, in other words, that the dissociative ion cluster mobilities are greatly different, thus supporting the earlier discussion. In fact, it is the OH^- ions (Eq 3) that are small, fast, and mobile, offsetting the mobilities of the comparatively large, slow, and immobile $H^+(H_2O)_c$ ions in determining the measured ion content of a vapor sample by electrical conductivity. Actual measured values of I_{cc} are shown in figure 2 vs Celsius temperature on the abscissa.[29] The upper curve shows the total ion population measured for fully saturated vapor (s = 1), while the lower diagonal curves show measured values of I_{cc} for vapor samples of constant partial pressure at several temperatures.

Data like those in figures 1 and 2 can be combined with Eq 6 to yield directly the total population of neutral clusters per cubic centimeter of vapor, N_{cc}, vs saturation ratio (= %RH/100) and temperature for vapor in contact with liquid water at equilibrium, as shown in figure 3. This figure shows that at any constant temperature (diagonals), N_{cc} has an $(s)^2$ dependency, i.e., a pressure-squared dependency just like that of the IR continuum absorption.[13] Figure 3 also shows that when a vapor sample is heated at constant partial pressure and progressively lower saturation ratios result, the value of N_{cc} remains virtually unchanged, as shown by the hozizontal line at $N_{cc} = 10^{15}$. This indicates that N_{cc} is a constant for a given partial pressure of water vapor at 1 atm total pressure, at least for conditions to the left of the nearly vertical diagonal in figure 3, which terminates at the boiling point. The significance of this nearly vertical diagonal will be discussed in the appendix.

Clearly, the IR, or other electromagnetic absorption due to molecular clusters of water in the atmosphere, will be proportional to the total cluster population per cubic centimeter, N_{cc}, *times* the mean size of the neutral cluster distribution, c_u.[10] N_{cc} is given directly for a wide range of conditions in figure 3. Values of c and c_u have been measured for many temperatures and partial

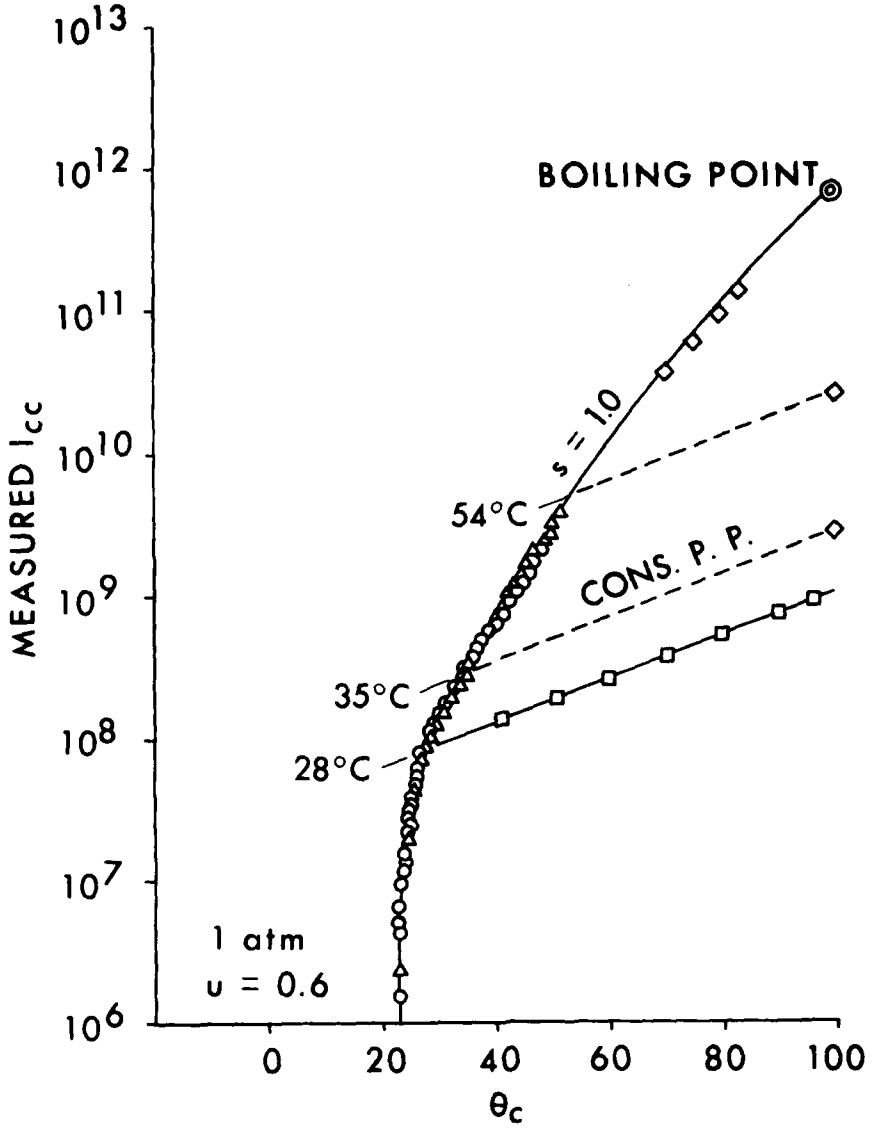

Figure 2. Measured Values of the Total Population per cc, I_{cc}, of Dissociative Ions of Neutral Water Clusters After Eq 3

The circular and triangular points are taken directly from electrical conductivity data, while the diamond and square points are obtained by calculation from mass spectral data. Ion mobility was taken as u = 0.6 cm^2/V-sec, and data are for 1 atm total pressure in moist air. Three constant-partial-pressure curves are shown, having shallower slopes than the saturation (s = 1.0) curve. These three curves correspond to heating saturated moist air (s = 1.0) to the temperatures shown from a starting temperature of (top to bottom) 54°C, 35°C and 28°C.

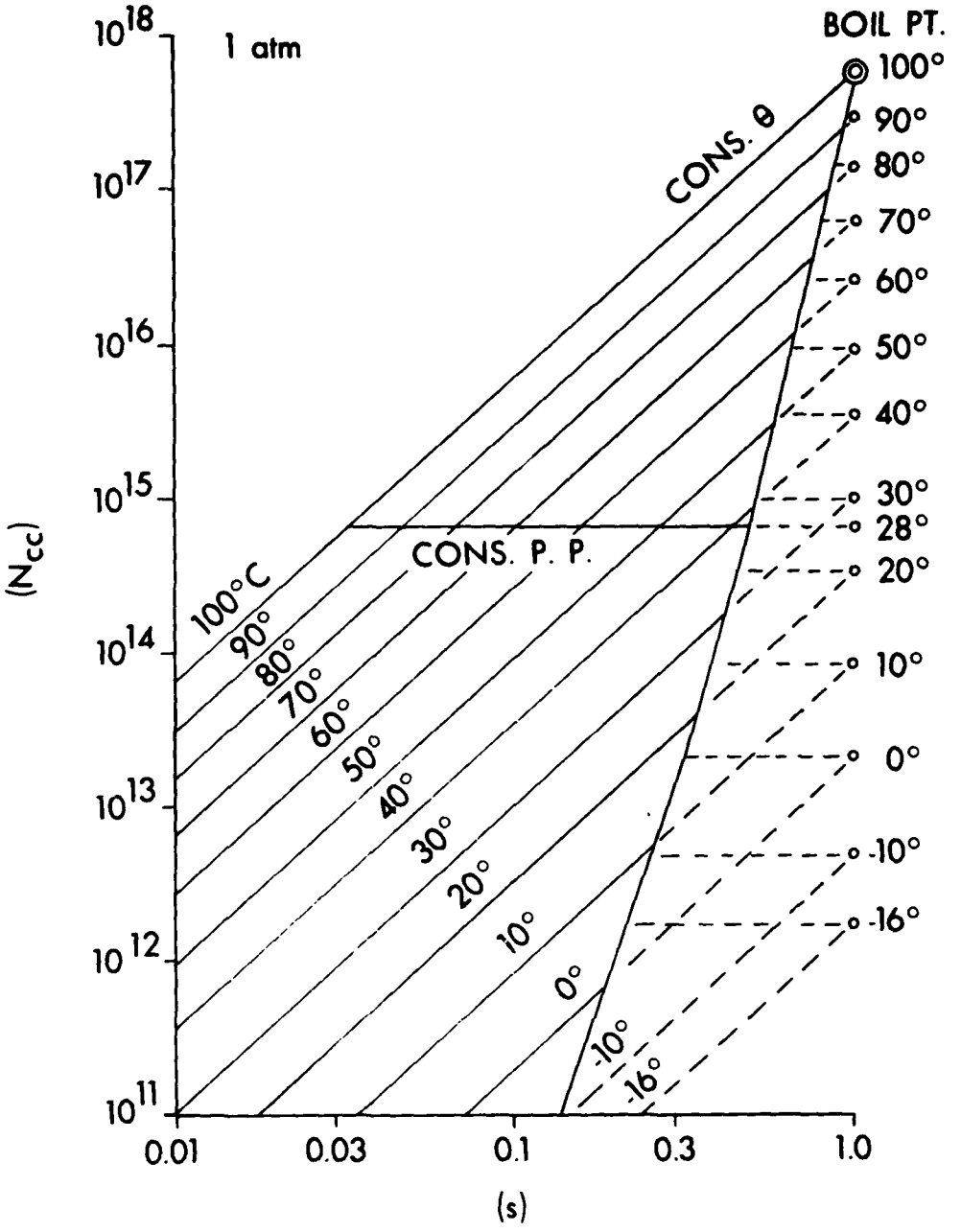

Figure 3. Total Population per cc of Neutral Water Clusters, N_{cc}, Obtained from Experimental Data for Ion Population, Equilibrium Constants and IR Absorption

Computed using Eq 6 from data like those in figures 1 and 2; the horizontal line represents constant partial pressure, while the nearly vertical curve to the right is explained in the appendix.

pressures by taking mass spectra[10] of moist air like those shown in figure 1. Thus if the total fraction of all water vapor that is clustered is designated as $(n_c)_v$, it is straightforward that:

$$(n_c)_v = \frac{(N_{cc})(c_u)}{N_1} \tag{7}$$

where N_1 is the population of monomers per cubic centimeter and is given by:

$$N_1 = \frac{(s \cdot p^\circ)\, N_{Avo}}{R\,\theta} \tag{8}$$

where R is the gas constant = 62,360 cc-Torr/°K g-mole (a Torr is a mm Hg), θ is the Kelvin temperature, $(s \cdot p^\circ)$ is the saturation ratio times the saturation vapor pressure (Torr) at this temperature, and, hence, the partial water vapor pressure (torr) and N_{AVO} is Avogadro's number = 6.02×10^{23} molecules per g-mole.

2.2 Data Interpretation from the New Theory.

Nonlinear data from many kinds of measurements can be explained by the new theory. Some examples include:

2.2.1 Infrared absorption measurements produce nonlinear results at higher saturations such as those seen by Bignell.[15] Spectral absorption data both in the IR and at millimeter- and micro-wavelengths[5,6] are extremely hard to reproduce, especially in humid climates. Measurements in steam[16,17] show different absorption behavior of water vapor than that seen at lower humidities, with sudden changes in spectral shapes, luminescence-like activity, and evidence that a very large fraction of the vapor, perhaps several percent or more, is clustered.[7] Vapor spectra taken with droplets present (thus assuring intimate vapor/liquid interaction with large interfacial areas to allow continuous evaporation and recondensation) show intense spectral activity that could be attributed to neutral clusters, especially in the millimeter-wave region[18] where droplet scattering is not confused with absorption.

2.2.2 In-house measurements of mass spectra of moist air[10] showed that samples for analysis at 99-100°C could only be obtained by drawing saturated water vapor into the mass spectrometer from flasks heated to a maximum temperature of 85-90°C. Attempts to use warmer saturated vapor, or to directly approach saturation at 99-100°C in the mass spectrometer sample volume, produced spectra for which the larger cluster sizes in the distribution (c = 45-50) no longer gave smooth, Gaussian-like distributions but very ragged ones. This allowed the interpretation that nucleation of the clusters of sizes 45-50 was occurring near the boiling point, a situation not allowed for by classical nucleation theory[20] which requires a so-called "critical supersaturation," $(s)_{crit}$, of ~1.9 for neutral cluster nucleation to form droplets near 100°C.

2.2.3 My measurements of I_{cc} (figure 2) showed that enormous total ion populations were possible, at temperatures approaching 100°C, of nearly 10^{12} per cubic centimeter.[29] These ion populations were sufficient (Eq 6) to account for *all* monomers at the boiling point and 1 atm total atmospheric pressure. Furthermore, when ion populations were measured at ambient temperature and lower saturation ratios, they increased linearly with s, i.e., with an s^1 power dependency, until a

saturation ratio of 0.5-0.6 (50-60% RH) was reached. At this point, Icc values measured vs s began to increase markedly, producing a sharp knee in the data curves that gave the appearance that I_{cc} had encountered some sort of diagonal barrier and was attempting to climb along it as s was increased further.[29]

2.2.4 The kinetic theory of evaporation and recondensation[35] for water at the vapor/liquid interface requires, to account for equilibrium evaporation rates actually measured for water, a saturation ratio of s = 0.99999+ at the evaporative boundary layer under virtually all conditions. This implies that at the boundary layer, the vapor and liquid phases are not clearly distinguishable and that, since liquid water is nearly completely hydrogen-bonded;[36] the vapor could be also. This could also account for the experimental observation that the dissociative ion product of water (Eq 5) applies to either the vapor or liquid phase. Croxton[37] states that no statistical-mechanical treatment of the vapor/liquid interface is yet reliable, and that water presents a particularly formidable problem in its interfacial properties.

The mean size, c_u, of the neutral cluster distribution increases with increasing s at constant temperature,[10] but under conditions of constant partial pressure, c_u can be described as a function of temperature alone. From experimental mass spectra, the equation of c_u is (see appendix):

$$(c_u)_{s,\theta} = (s \cdot p^{\circ}_{\theta})^{1/2} \exp(1919/\theta - 4.655), \tag{9}$$

while the general equation for the ratio of c_u's for two conditions is:

$$\frac{(c_u)_2}{(c_u)_1} = \left(\frac{s_2 p^{\circ}_2}{s_1 p^{\circ}_1}\right)^{1/2} \exp \tau\,(1/\theta_2 - 1/\theta_1) \tag{10}$$

where in this case τ = 1919.

Consequently, the negative temperature dependency of the IR continuum absorption, e.g., could be determined by the negative temperature dependency of the mean cluster size at constant partial pressure. If one wishes to assume a Boltzmann-like temperature dependency for c_u, hydrogen bond energies on the order of -0.1 to -0.2 ev from Eq 9 will be computed. Results of such magnitude often have been reported by spectroscopists who assumed that the dimer (cluster of size c = 2) alone accounted for anomalous absorption by atmospheric water vapor,[6] but they assumed that it was the population of dimers, not the cluster size, that had this dependency.

From Eq 7, the total cluster fraction $(n_c)_v$ equals the product of (N_{cc}) times c_u divided by the monomer population, N_1. Actual values and ratios of c_u are given in Eqs 9 and 10. From experimental measurements, the equations of N_{cc} also are known (figure 3):

$$(N_{cc})_{s,\theta} = 1.056 \times 10^{12} (s \cdot p^{\circ}_{\theta})^2 \tag{11}$$

and thus the general equation for the ratio of N_{cc}'s for two conditions is:

$$\frac{(N_{cc})_2}{(N_{cc})_1} = \left(\frac{s_2 p_2^\circ}{s_1 p_1^\circ}\right)^2 \tag{12}$$

which is constant at constant partial pressure. By combining Eqs 10 and 12, the general equation for the ratio of the product $(Ncc)(c_u)$ for two conditions is obtained:

$$\frac{(N_{cc})_2 (c_u)_2}{(N_{cc})_1 (c_u)_1} = \left(\frac{s_2 p_2^\circ}{s_1 p_1^\circ}\right)^{5/2} \exp \tau\,(1/\theta_2 - 1/\theta_1) \tag{13}$$

From Eq 7, the general equation for the ratio of total cluster fraction for two conditions is:

$$\frac{(n_c)_{v2}}{(n_c)_{v1}} = \left(\frac{s_2 p_2^\circ}{s_1 p_1^\circ}\right)^{3/2} \frac{\theta_2}{\theta_1} \exp \tau\,(1/\theta_2 - 1/\theta_1) \tag{14}$$

3. THE INFRARED CONTINUUM ABSORPTION

The neutral cluster species for which detailed physical descriptions have been given earlier would always exist in the atmosphere, and when in equilibrium with liquid water they would be found in the populations and sizes given in figures 1 and 3. These neutral clusters would interact with electromagnetic radiation at all wavelengths, to a greater or lesser extent, owing to the different kinds of cluster modes in different spectral regions. While the following discussion will focus on the IR continuum absorption because the IR is the spectral region best known to me, a treatment similar to the following could be used by spectroscopists in other wavelength regions to model cluster activity in the atmosphere.

Since the electromagnetic absorption at any wavelength due to neutral clusters in the vapor will be directly proportional to the product of cluster population, N_{cc}, times average size, c_u, (Eq 7) which is proportional to the fraction of the vapor clustered, $(n_c)_v$, it follows that:

$$\frac{\alpha_{v_2}}{\alpha_{v_1}} = \frac{(n_c)_{v_2}}{(n_c)_{v_1}} \tag{15}$$

where α_v is a mass absorption coefficient having units like cm^2/g or m^2g. Thus, the ratio of α's in Eq 15 also is equal to the right-hand side of Eq 14. Furthermore, the so-called self-broadening coefficient, (C_s°), of the IR continuum absorption is related to α by:

$$\frac{(C_s^\circ)_2}{(C_s^\circ)_1} = \frac{\alpha_{v_2}}{\alpha_{v_1}} \left(\frac{s_1 p_1^\circ}{s_2 p_2^\circ}\right) \tag{16}$$

where (C_s°) has the units cm2/monomer-atm. Thus combining Eqs 14, 15, and 16 gives, at some specified wavelength λ (μm):

$$\left[\frac{(C_s^\circ)_2}{(C_s^\circ)_1}\right]_\lambda = \left(\frac{s_2 p_2^\circ}{s_1 p_1^\circ}\right)^{1/2} \frac{\theta_2}{\theta_1} \exp \tau\,(1/\theta_2 - 1/\theta_1) \qquad (17)$$

Eq 17 is similar to one proposed by Roberts *et al.*,[19,13] to model the temperature dependency observed experimentally for $(C_s^\circ)_\lambda$ when the reference temperature $\theta_1 = 296^\circ$K:

$$(C_s^\circ)_{\lambda,\theta} = (C_s^\circ)_{\lambda,296} \exp \tau_o\,(1/\theta_2 - 1/296) \qquad (18)$$

However, Eq 18 omits all of the pressure and temperature terms to the left of the exp term in Eq 17. This suggests that Eq 18 is correct only under certain circumstances, i.e., when near-constant partial pressure is maintained between two temperatures with only a slight pressure variation needed to offset the ratio of absolute temperatures. We can examine this by plotting Eqs 17 and 18 together, for $\tau = \tau_o = 1919$, as is done in figure 4. Eq 17 produces the field of curves shown when referenced to 23°C (Roberts *et al.*, 296°K). The reference point in figure 4 is shown at $s = 0.457$, which is on the right-hand diagonal discussed in the appendix. Figure 4 includes dashed curves showing Eq 18 and also constant partial pressure conditions. The interpretation is borne out that Eq 18 works only for ~ constant partial pressure (probably due to the manner in which experiments were run from which it was derived), while Eq 17 is general and should work very well for all combinations of water vapor partial pressure and temperature in the real atmosphere.

In an earlier paper,[13] I gave an equation that can model the behavior of figure 4 because it is based on the dissociative ion product of water (Eq 5):

$$(C_s^\circ)_{\lambda,\theta_2} = (C_s^\circ)_{\lambda,\theta_1} \left(\frac{s_1}{s_2}\right)^m \left(\frac{p_{w_1}^\circ}{p_{w_2}^\circ}\right)^n \exp[3578\,(1/\theta_1 - 1/\theta_2)] \qquad (19)$$

Now it is possible to solve for the exponents m and n in Eq 19 simply by setting this equation equal to Eq 17, from which, exactly:

$$m = -1/2 \qquad \text{and} \qquad n = 1/2$$

and thus the general equation for figure 4 also can be given by:

$$\left[\frac{(C_s^\circ)_2}{(C_s^\circ)_1}\right]_\lambda = \left(\frac{s_2 p^\circ_1}{s_1 p^\circ_2}\right)^{1/2} \exp 3578\,(1/\theta_1 - 1/\theta_2) \qquad (20)$$

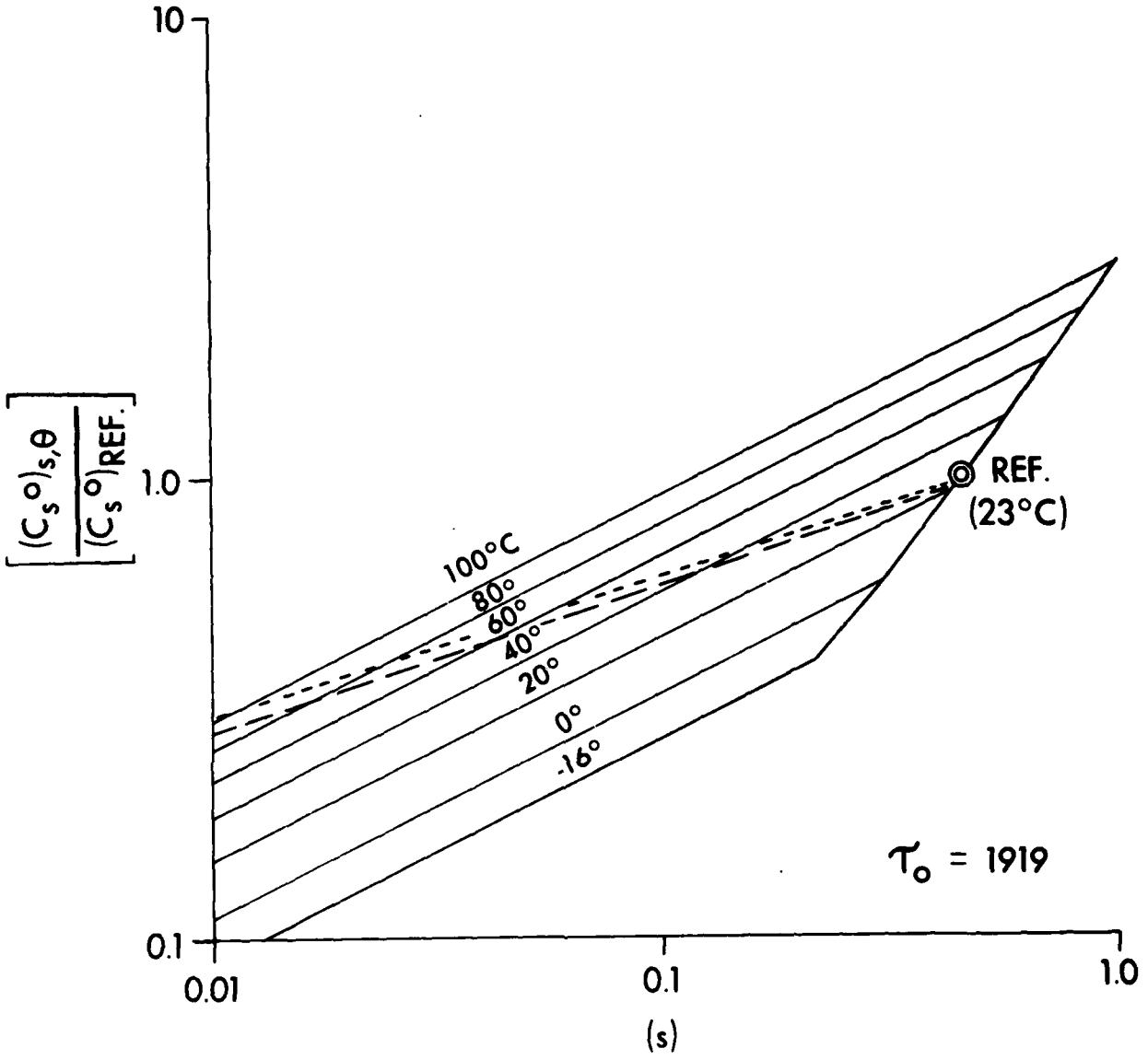

Figure 4. Plot of Eqs 17 and 18 for $\tau = \tau_o = 1919$

Eq 17 produces the field of curves but Eq 18 produces only the long-dashed curve that approximates constant partial pressure conditions shown by the short-dashed curve; reference conditions are 296°K and the value $(s)_{bar} = 0.457$ on the diagonal as discussed in the appendix.

which for constant partial pressure gives:

Constant Partial Pressure

$$\left[\frac{(C_s^\circ)_2}{(C_s^\circ)_1}\right]_\lambda = \frac{p^\circ_1}{p^\circ_2} \exp 3578\,(1/\theta_1 - 1/\theta_2) \tag{21}$$

Eq 21 justifies exactly the original observation[8,9,13] that $(C_s^\circ)_\lambda$ is directly proportional to the ion product as $\sqrt{K_w}$ (Eqs 5 and 6) divided by pressure:

$$(C_s^\circ)_\lambda = \frac{k\sqrt{K_w}}{p_w} \tag{22}$$

where $p_w = p^\circ_w$, and the ratio of (C_s°)'s is given in Eq 21 since[13]

$$\sqrt{K_w} = \exp\left(\frac{-3578}{\theta} - 4.085\right) \tag{23}$$

For comparison with Eq 18, which is referenced to 296°K, Eq 20 can be written:

$$(C_s^\circ)_{s,\theta} = \left(\frac{s}{p^\circ}\right)^{1/2} \exp\,(14 - 3578/\theta) \tag{24}$$

in general form; or for constant partial pressure in the form:

Constant Partial Pressure, $$(C_s^\circ)_\theta = \frac{1}{p^\circ} \exp\,(15.14 - 3578/\theta) \qquad 296°K: \tag{25}$$

Eqs 24 and 25 will reproduce the curves of figure 4 quite precisely. All of the equations given in this section can, of course, be written to reference any temperature from -16°C to 100°C, the limits of vapor/liquid equilibria at 1 atm.

The diagonal curve shown in figure 4 and discussed in the appendix has been mentioned previously. If one humidifies a sample and thus increases s, for example at constant temperature, it can be seen that when the diagonal is reached the measured values of (C_s°) vs s will turn sharply upward. This will lead the spectroscopist to believe that he has caused condensation to occur on his optics or, if the optics are heated, that droplet growth has begun on conventional condensation nuclei, making his data useless. In reality what has happened is that the nuetral cluster population (figure 3) increases more rapidly with s under these conditions. The data obtained by the spectroscopist will be perfectly legitimate cluster absorption data, but will be confused with conventional interpretations that droplets are present and are scattering or absorbing radiation. But the clusters themselves will grow into droplets if allowed to nucleate. The existence of clusters and droplets together is not only explicable by the new theory, it is indeed inescapable.

Regardless of wavelength, the anomalous absorption of water vapor can be attributed to modes of hydrogen-bonded molecular clusters like those found in the liquid phase which are present as fractions, $(n_c)_v$, of the vapor given in several equations in this paper. But only some fraction, which can be called $(n_g)_\lambda$, of $(n_c)_v$, will be active in the absorption at some wavelength λ. Spectra of steam[17] give clues about the wavelength-dependency of absorption produced by the neutral cluster distributions in vapor like those in figure 1. For example, at 400°K data like those in figure 5 are obtained. Earlier analyses have shown that for a variety of cluster configurations some modes of the clusters should be resonant at wavelengths such that:[8,9]

$$\lambda = 6.4\sqrt{c} \tag{26}$$

This seems to be borne out in figure 5, where the four vertical lines correspond to wavelengths, reading from left to right, of cluster sizes in Eq 26 of c = 3, 4, 5, 6. But note also that the amplitudes of the recognizable peaks, which are spaced properly *only* for a constant of 6.4 in Eq 26, are only a small fraction of the amplitude of the overall envelope of the IR continuum absorption. This suggests that the modes responsible for the relationship in Eq 26 are only some of those responsible for the overall absorption or, at the very least, that the individual cluster resonances give rise to absorption bands that are so broad that they overlap those of many neighbors and, therefore, that the continuum absorption envelope adds together the "wings" of many bands or lines. Eq 26 turns out in practice to be very useful, and it can be easily shown that spectra computed by it from cluster distributions match the continuum. The overall absorption will be proportional to the product of N_{cc}, c_u, and an average absorption coefficient due to hydrogen-bonded monomers in the vapor that can be designated $(\alpha_H)_\lambda$ and can be given the units cm^2/clustered molecule. There is no reason to believe that this absorption coefficient cannot be calculated from the known spectral properties of liquid water at wavelength λ, because the clustered molecules are like those found in liquid water. If one treats the clusters in vapor as tiny aerosols, it follows that their average absorption coefficient can be computed from:[11]

$$(\alpha_H)_\lambda = \frac{4\pi \times 10^4 k_\lambda f(m_\lambda) M}{\lambda \rho (n_c)_L N_{Avo}} \tag{27}$$

where k_λ is the imaginary part of the complex index of refraction $(n - ik)_\lambda = m_\lambda$, for water at wavelength λ, M = 18 is the molecular weight, N_{Avo} is Avogadro's number, $\rho \sim 1.0$ is the liquid water mass density (g/cc), $(n_c)_L$ is the fraction of liquid water clustered at the temperature of interest ($\sim$0.85 at 20°C)[36], and f(mλ) is given by:

$$f(m_\lambda) = \left[\frac{9n}{(n^2 + k^2)^2 + 4(n^2 - k^2) + 4}\right] \tag{28}$$

where n_λ is the real part of the complex index of refraction. Very precise values of n_λ and k_λ have been given by Hale and Querry.[38] For many approximation calculations, one can take $f(m_\lambda) \sim 1.0$. From the above equations and assumptions it follows that the absorption coefficient of water vapor that can be attributed to neutral clusters (Bignell's "k_2"[15]), $(\alpha_v)_{\lambda,\theta}$ (cm^2/g) is:

$$(\alpha_v)_{\lambda,\theta} = \frac{4\pi \times 10^4 (n_g)_\lambda (s \cdot p^\circ) k_\lambda f(m_\lambda)}{\lambda \cdot \rho \cdot (1)(760)(n_c)_L} \tag{29}$$

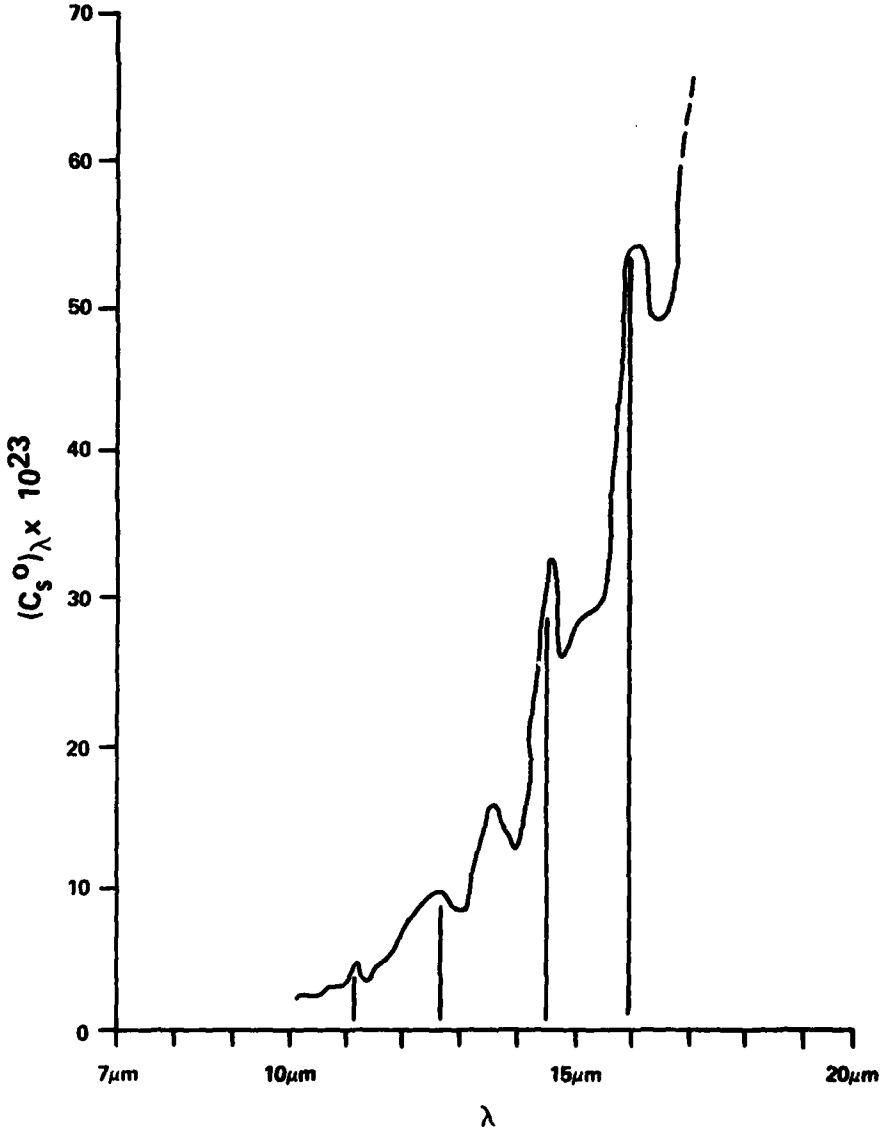

Figure 5. Steam Data from Ref. 17 Showing Features in the Self-Broadening Coefficient Spectrum $(C_S^\circ)_\lambda$ Spaced According to the Simple Relationship of Eq 26

Hence, the "self-broadening" coefficient of the IR continuum absorption is:

$$(C_s^\circ)_\lambda = \frac{M(1)(760)}{N_{Avo}(s \cdot p^\circ)_\theta} \cdot (\alpha_v)_{\lambda,\theta} = 4\pi \times 10^4 (n_g)_\lambda \frac{M k_\lambda f(m_\lambda)}{N_{Avo} \lambda \rho (n_c)_L} \quad (30)$$

Roberts *et al.*[19] have given a useful equation for the spectral dependency of the IR continuum absorption which can be rewritten for wavelength instead of wavenumber as:

$$(C_s^\circ)_{\lambda,296} = 10^{-22}\left[1.25 + 1670 \exp\left(\frac{-78.7}{\lambda}\right)\right] \quad (31)$$

for θ = 296°K. Using Eq 31 with Eq 30 and taking $\rho = f(m\lambda) = 1.0$, one can calculate the fraction of $(n_c)_v$ that is active in the absorption at wavelength λ, i.e., $(n_g)_\lambda$. The result for 296°K is shown in figure 6. The results are consistent with the earlier observation that, even in stream, the fraction of IR absorption/emission attributable to cluster modes active near λ = 10 um is only a few percent,[7] even though nearly all water vapor is clustered near the boiling point. Near the peak of the IR continuum absorption beyond λ = 30 μm, figure 6 indicates that almost all clustered molecules contribute to this absorption.

But there is no need to show that the entire continuum absorption through the rotational band at 30-50 μm is due to clusters. Much of this absorption, especially at longer wavelengths, can be attributed to monomer modes. Thus there are alternative explanations ot the ranging of $(n_g)_\lambda$ over so large a range of magnitudes as is shown in figure 6, although the evidence is considerable that this approach is valid in the continuum absorption wavelengths ranging at least from 8 to about 20 μm.

4. CONCLUSIONS

The work discussed has shown that anomalous electromagnetic absorption, at least in the IR continuum absorption wavelength region, can be quantitatively described as being due to distributions of neutral molecular clusters in water vapor and moist air whose populations, sizes, dependencies on humidity and temperature, and other parameters, also have been modeled here. The ratio modeling equations (Eqs 12-17 and 19-21) produce results in excellent agreement with observation and show the complete range of variation in response to s and θ, not just the absorption at constant partial pressure as approximated, for example, by Eq 18. These new equations are based on the physics of water vapor and, therefore, they should permit improved modeling of atmospheric IR transmission. They are recommended for evaluation by experimentalists and for inclusion in existing atmospheric transmission models as warranted. Since the cluster species believed responsible for anomalous electromagnetic absorption are well described, it should be possible for workers in other wavelength regions than the IR, e.g., in millimeter waves and microwaves, to compute and to experimentally verify absorption attributable to modes of neutral clusters active in the absorption at those wavelengths.

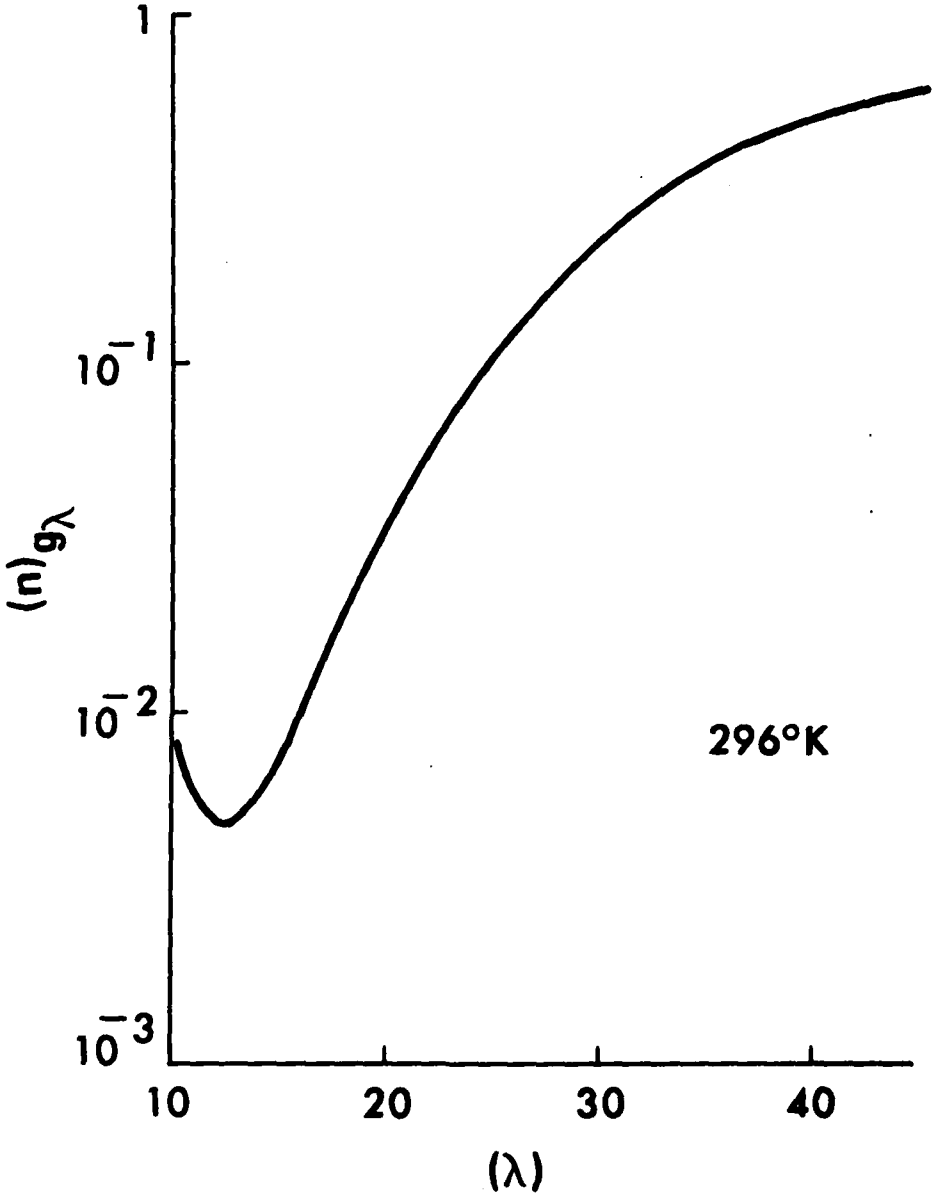

Figure 6. Fraction, $(n_g)_\lambda$, of the Total Cluster Fraction in Vapor, $(n_c)_v$, Active in the IR Continuum Absorption vs Wavelength λ

Computed from Eq 30 using $(C_s^\circ)_\lambda$ values from Eq 31.

LITERATURE CITED

1. Carlon, H. R. The Apparent Dependence of Terrestrial Scintillation Intensity Upon Atmospheric Humidity. Appl. Opt. *4*, 1089-1097 (1965).

2. Carlon, H. R. Humidity Effects in the 8-13μ Infrared Window. Appl. Opt. *5*, 879 (1966).

3. Carlon, H. R. Infrared Emission by Fine Water Aerosols and Fogs. Appl. Opt. *9*, 2000-2006 (1970).

4. Carlon, H. R. Model for Infrared Emission of Water Vapor/Aerosol Mixtures. Appl. Opt. *10*, 2297-2303 (1971).

5. Carlon, H. R. Phase Transition Changes in the Molecular Absorption Coefficient of Water in the Infrared: Evidence for Clusters. Appl. Opt. *17*, 3192-3193 (1978).

6. Carlon, H. R. Molecular Interpretation of the I.R. Water Vapor Continuum: Comments. Appl. Opt. *17*, 3193-3195 (1978).

7. Carlon, H. R. Variations in Emission Spectra from Warm Water Fogs: Evidence for Clusters in the Vapor Phase. Infrared Phys. *19*, 49-64 (1979).

8. Carlon, H. R. Ion Content and Infrared Absorption of Moist Atmospheres. J. Atmos. Sci. *36*, 832-837 (1979).

9. Carlon, H. R. Do Clusters Contribute to the Infrared Absorption Spectrum of Water Vapor? Infrared Phys. *19*, 549-557 (1979).

10. Carlon, H. R., and Harden, C. S. Mass Spectrometry of Ion-Induced Water Clusters: An Explanation of the Infrared Continuum Absorption. Appl. Opt. *19*, 1776-1786 (1980).

11. Carlon, H. R. Aerosol Spectrometry in the Infrared. Appl. Opt. *19*, 2210-2218 (1980).

12. Carlon, H. R. Mass Spectrometry of Ion-Induced Water Clusters: An Explanation of the IR Continuum Absorption; Addenda.. Appl. Opt. *20*, 726-727 (1981).

13. Carlon, H. R. Infrared Water Vapor Continuum Absorption: Equilibria of Ions and Neutral Water Clusters. Appl. Opt. *20*, 1316-1322 (1981).

14. Carlon, H. R. Infrared Absorption by Molecular Clusters in Water Vapor. J. Appl. Phys. *52*(5), 3111-3115 (1981).

15. Bignell, K. J. The Water-Vapour Infra-Red Continuum. Q. J. R. Meteorol. Soc. *96*, 390-403 (1970).

16. Elsasser, W. M. Note on Atmospheric Absorption Caused by the Rotational Water Band. Phys. Rev. *53*, 768 (1938).

17. Varanasi, P., Chou, S., and Penner, S. S. Absorption Coefficients for Water Vapor in the 600-1000 cm^{-1} Region. J. Quant. Spectrosc. Radiat. Transfer *8*, 1537-1541 (1968).

18. Emery, R. J., Zavody, A. M., and Gebbie, H. A. Measurements of Atmospheric Absorption in the Range 5-17 cm^{-1} and Its Temperature Dependence. J. Atmos. and Terres. Phys. *42*, 801-807 (1980).

19. Roberts, R. E., Selby, J. E. A., and Biberman, L. M. Infrared Continuum Absorption by Atmospheric Water Vapor in the 8-12 μm Window. Appl. Opt. *15*, 2085-2090 (1976).

20. Wilson, J. G. Principles of Cloud Chamber Technique. Cambridge University Press, London. 1951.

21. Wilson, C.T.R. Philos. Trans. (London) *189*, 265 (1897).

22. Wilson, C.T.R. Philos. Trans. (London) *192*, 403 (1899).

23. Pauling, L. The Structure of Water. p1, Chap. 1. Hydrogen Bonding. D. Hadzi, ed. Pergamon Press, New York, New York. 1959.

24. Carlon, H. R. Ion Content of Air Humidified by Boiling Water. J. Appl. Phys. *51*(1), 171-173 (1980).

25. Carlon, H. R. Ionic Equilibria and Decay Times of Neutral Water Clusters in Moist Air. J. Appl. Phys. *52*(3), 1584-1586 (1981).

26. Carlon, H. R. Equilibrium Ion Content of Water Vapor in Air. J. Appl. Phys. *52*(4), 2638-2641 (1981).

27. Carlon, H. R. Limits of Detection for Condensation Nuclei Counters. J. Appl. Phy Phys. *52*(4), 3062-3063 (1981).

28. Israel, H. Atmospheric Electricity. Israel Program for Scientific Translations, Jerusalem, Israel. Vol. 1 (1971).

29. Carlon, H. R. New Measurements of the Ion Content of Evaporation-Humidified Air, accepted by J. Chem. Phys. (est. May 1982).

30. Prutton, C. F., and Maron, S. H. Physical Chemistry. p 367. Macmillan Book Co. New York, New York. 1951.

31. Koref, F. Z. anorg. Chem. *66*, 73 (1910).

32. Kassner, J. L., Jr., and Hagen, D. E. Comment on Clustering of Water on Hydrated Protons in a Supersonic Free Jet Expansion. J. Chem. Phys. *64*, (letters section), 1860-1861. 15 Feb (1976).

33. Searcy, J. Q., and Fenn, J. B. Clustering of Water on Hydrated Protons in a Supersonic Free Jet Expansion. J. Chem. Phys. *61*, 5282-5288 (1974).

34. Lee, N., Keesee, R. G., and Castleman, A. W., Jr. On the Correlation of Total and Partial Enthalpies of Ion Solvation and the Relationship to the Energy Barrier to Nucleation. J. Colloid and Interface Sci. *75*, 555-565 (1980).

35. deBoer, J. H. The Dynamical Character of Adsorption. p16. Oxford Press, Clarendon, England. 1953.

36. Luck, W.A.P. Water: A Comprehensive Treatise. p 210, Vol. 1. F. Franks, ed. Plenum Press, New York, New York. 1972.

37. Croxton, C. A. Statistical Mechanics of the Liquid Surface. Wiley Interscience. New York, New York. 1980.

38. Hale, G. M., and Querry, M. R. Optical Constants of Water in the 200-nm to 200-μm Wavelength Region. Appl. Opt. *12*, 555-563 (1973).

APPENDIX

MICROPHYSICS OF CLOUDS AND NUCLEATION THEORY

The following discussion is not essential to the development of the equations given in the text, which are obtained directly from experimental data discussed there. This appendix is included for readers interested in the microphysics of clouds and nucleation theory (gas to particle conversion), since the interpretations presented here can be supported by the various experimental data but are decidedly contrary to existing theories. The agreement between these interpretations and observation remind us that any theory is only as good as its agreement with the data. This includes traditional theories, however ingrained in our thinking they may have become with the passage of time. The reader is encouraged to consider these arguments open-mindedly. If large populations of neutral molecular clusters exist in water vapor, they surely must serve as condensation sites for the growth of droplets under suitable conditions. Thus there would be no need to explain these sites as originating from monomer collisions according to classical kinetic theory, which in any case is imprecise for the vapors of hydrogen-bonded substances like water. In this section, an alternative explanation is given which fits all observations, but for which no further justification is claimed.

Mass spectra and other measurements require that the possibility be considered that, at the boiling point, critical conditions are attained and nucleation and recondensation occur continuously between the vapor and liquid phases of water. If essentially all vapor is clustered at the vapor/liquid interface at the boiling point (s = 1.0, 100°C, 1 atm), then the *maximum* partial pressure fraction for freshly evaporated water vapor at the liquid interface at 1 atm under other conditions than the boiling point is:

$$(n_c)_v = \frac{(s)(p^\circ_\theta)}{(1)(760)} \qquad \text{(A-1)}$$

where s is the saturation ratio and p° is the saturation vapor pressure at temperature θ.

This simple equation, with standard vapor pressure tables, allows the construction of what might be called equilibrium phase diagram for vapor-phase clusters in contact with liquid water, as drawn in figure A-1, for 1 atm total pressure. The values of $(n_c)_v$ given by Eq A-1 and shown in figure A-1, are found to be in good agreement with estimates of the cluster fraction from measurements discussed in the text, provided that liquid water is present in the system. Since by this interpretation all excess vapor must be condensed at s = 1.0, a vertical condensation line is shown there. Figure A-1 shows that a surprisingly large fraction of water vapor is clustered even at temperatures and humidities well below the boiling point, provided that liquid water is present in the system and is in equilibrium with the vapor. For example, one percent of all vapor can be clustered at 40°C for a saturation ratio s = 0.15 (15% RH). But this entire fraction, as discussed in the text, is not effective in absorption except near the peak of the IR continuum absorption spectrum (30-50 μm). Therefore measurements of electromagnetic radiation absorption by neutral water clusters in the atmosphere frequently infer that cluster populations, and hence the fraction of vapor clustered $(n_c)_v$, are smaller than actually is the case and can be demonstrated, e.g., by measurements of the dissociative ions of the neutral clusters by electrical conductivity. The diagonal line with points in figure A-1 and the dashed nearly vertical line now will be considered.

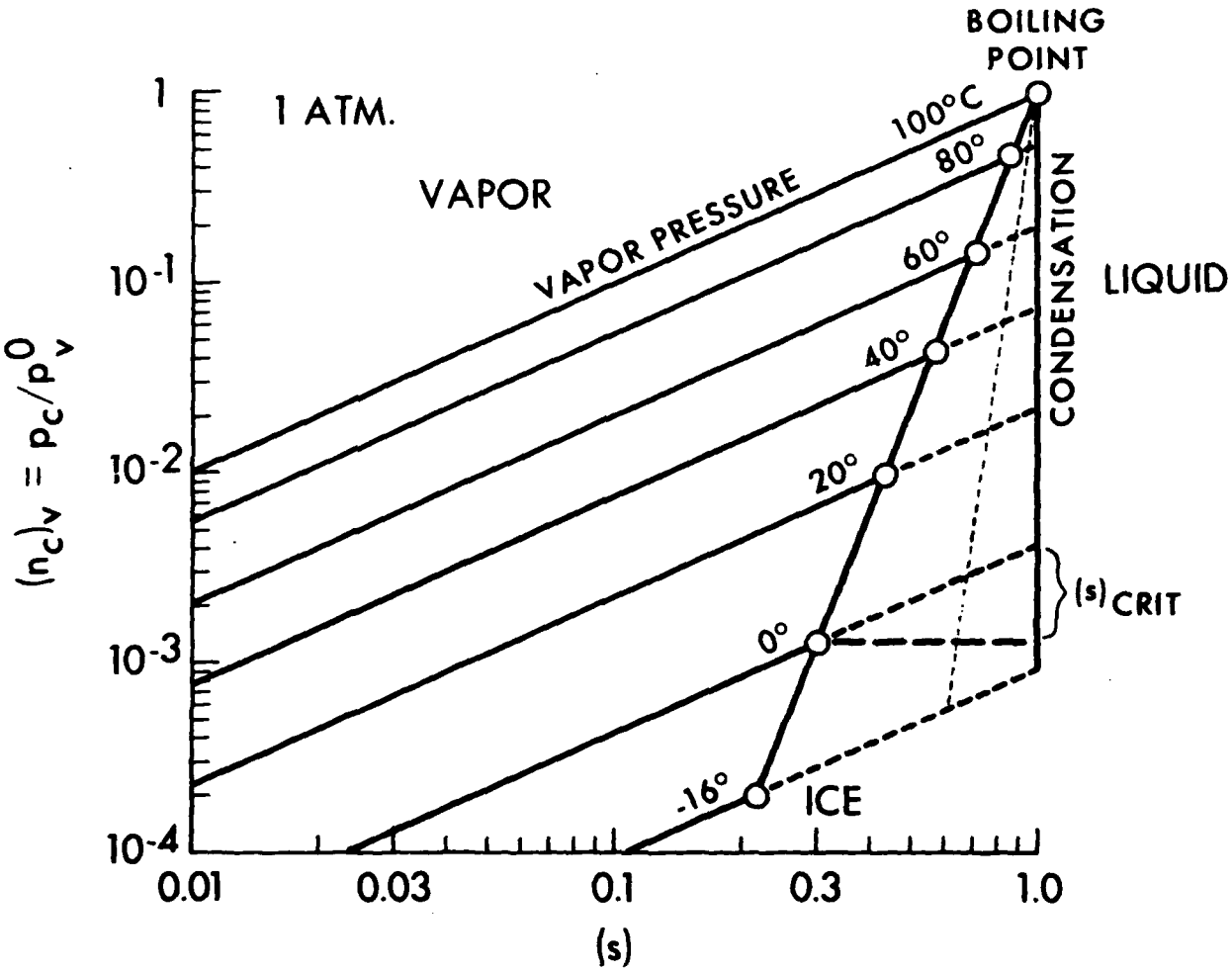

Figure A-1. Phase Diagram of Neutral Clusters Constructed from Eqs A-1 and A-2 and Standard Tables of Water Saturation Vapor Pressure According to the Methodology in the Appendix

If nucleation of neutral clusters in the vapor can occur at s = 1 (an assumption long made by atmospheric cloud macrophysicists, although without theoretical justification), then so-called supersaturation need not exist to explain nucleation, as all nucleation phenomena could be explained as temperature rather than partial pressure phenomena. Wilson,[1,2] had he known about hydrogen bonding and the existence of equilibrium neutral cluster populations in water vapor when his classical adiabatic expansion (cooling) cloud chamber experiments were performed, could have explained his results as due to changes in temperature alone. Saturation vapor pressure is a fundamental physical constant of water at any temperature, and the concept of exceeding it arbitrarily to explain new results by "supersaturations" of four or five must have caused concern. Indeed, Wilson had misgivings about his observations.[3] While many empirical modifications to nucleation models and equations have proved necessary over the years to secure good agreement between theory and cloud chamber observation, these modifications have served only to secure this agreement; they do not prove that the supersaturation concept is a correct one.

The interpretation of the boiling point as the critical saturation point leads to simple equations that are found to fit experimental data more closely than do traditional models based on supersaturation. For example, if one considers the temperature drop that is required to produce a certain excess of water vapor that is then available to condense on clusters to grow droplets large enough for optical detection,[4] then the "barrier" conditions that must be attained for droplet formation can be given as a simple function for *sub*saturated vapor referenced to the boiling point:

$$\text{"Barrier" Conditions: } \ln(s)_{bar} = 1 - \left(\frac{373}{\theta}\right)^{5/2} \qquad \text{(A-2)}$$

Eq A-2 is not unlike classical nucleation equations, but it gives exact solutions rather than approximate ones as in the equations of J. G. Wilson.[5] Eq A-2 is the diagonal line with points plotted in figure A-1, and its equivalent curve for N_{cc} corresponding to $(n_c)_v$ is shown as a nearly vertical function in figure 3 of the main body of this report. Eq A-2 also defines the right-hand diagonal of figure 4, in equivalent units for (C_s°). The dashed, nearly vertical line in figure A-1 is this barrier equation corrected for I_{cc} by using the temperature dependence of the ion product (Eqs 6, 23). When considering the neutral cluster fraction in water vapor or the cluster populations, N_{cc}, the solid barrier curve with points in figure A-1, therefore, is applicable.

Perhaps fortuitously, it is found that $(n_c)_v$ can be calculated almost precisely at the barrier curve by:

$$(n_c)_{v_{bar}} = \exp 10.55\left[1 - \left(\frac{373}{\theta}\right)^{3/2}\right] \qquad \text{(A-3)}$$

which requires that:

$$(n_c)_{v_{bar}} = \exp\left[1 + \ln\left(\frac{p^\circ}{760}\right) - \left(\frac{373}{\theta}\right)^{5/2}\right] \qquad \text{(A-4)}$$

And thus if one wishes to take the ratio of the fraction clustered at two temperatures other than 373°K, he obtains:

$$\left(\frac{(n_c)_{v_2}}{(n_c)_{v_1}}\right)_{bar} = \left(\frac{p^\circ_2}{p^\circ_1}\right)\exp\left[\left(\frac{373}{\theta_1}\right)^{5/2} - \left(\frac{373}{\theta_2}\right)^{5/2}\right] \qquad \text{(A-5)}$$

In figure A-2, Eq 9 is plotted to show the mean size of the neutral cluster distribution vs s and θ from the mass spectral data of Ref. 3 and the interpretations of the text. The barrier curve from Eq A-2 is included.

All of the examples of nonlinear data discussed in the text can be explained by the barrier curve of Eq A-2. IR absorption vs s becomes nonlinear as the barrier curve is approached due to nonlinear changes in the cluster population. Thus modelers must be careful to avoid saturation ratios approaching the barrier in their data collection, and spectroscopists could confuse barrier conditions as due to droplet growth on large, conventional condensation nuclei when in fact it was the cluster population that was responding to the barrier. This would be the true beginning of what might be called droplet growth, but it is distinctly different from that on other nuclei. It is the beginning of accelerated growth of homogeneous neutral clusters already present in the vapor, and it will occur regardless of whether other, larger condensation nuclei are present in the system or not, provided that liquid water is present. In steam, virtually all water vapor can be clustered, thereby explaining the enormous IR absorptions and emissions reported by many workers.[6-8] after monomer and droplet corrections are made. Observations since Faraday's time have shown that saturated steam contains enormous populations of (dissociative) ions, but that dry superheated steam has far fewer ions present. If temperatures above 100°C are to be investigated for cluster activity in water vapor, the total pressure must also be raised to maintain equilibrium conditions. Since the boiling point keys this activity, one might expect that water vapor samples run in partial vacuum will give variable results depending on cluster species and populations present. The dissociative ion populations (I_{cc}) closely track the neutral cluster populations (N_{cc}) in experimental measurements.

Conditions to the left of the diagonal barrier with points in figure A-1 are difficult to reproduce in the atmosphere because, if liquid water is present in the system, s will increase to the barrier while, if liquid is not present, the neutral cluster population will decay to lower, nonequilibrium $(n_c)_v$'s. A common atmospheric occurrence is that of approximately constant partial pressure with temperatures changing over a period of hours, leading to changes in the saturation ratio (relative humidity). Constant partial pressure is shown by the dashed horizontal line in figure A-2, and results in very small changes in $(n_c)_v$. Measurements of the ion population of atmospheric air show much lower I_{cc} values in aged moist air than in air recently in contact with liquid water.

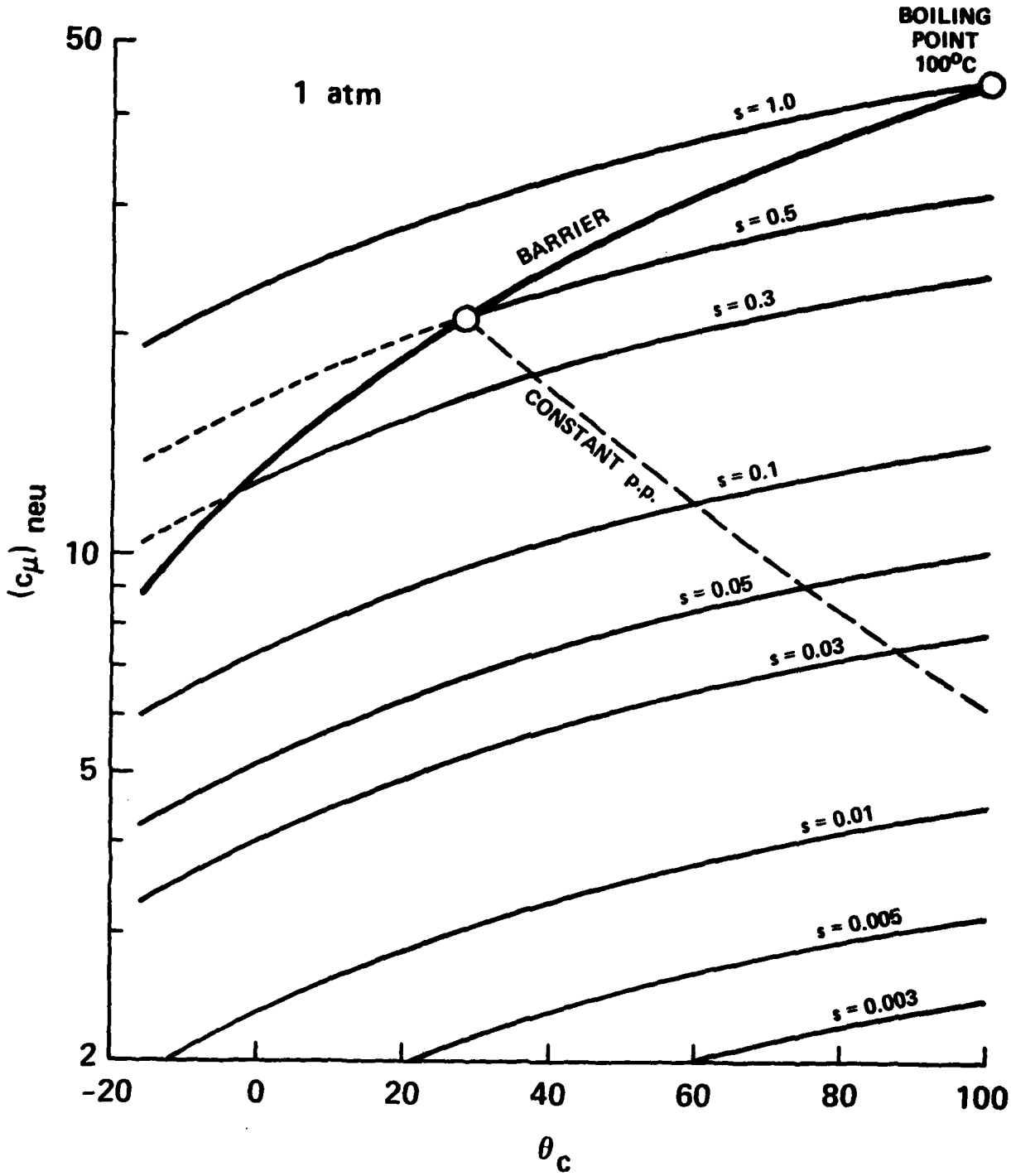

Figure A-2. Mean Size of the Neutral Cluster Population from Eq 9 Derived from Mass Spectral Data of Ref. 3

These are mean sizes only, and the full distributions include clusters of considerably smaller and larger numbers of monomers (c's). Sizes are estimated by adding 1 to the ion cluster measured sizes, per the discussion of Eq 3. The barrier equation curve (Eq A-2) is included for reference.

LITERATURE CITED

1. Wilson, C. T. R. Philos. Trans. (London). *189*. 265 (1897).

2. Wilson, C. T. R. Philos. Trans. (London). *192*, 403 (1899).

3. Carlon, H. R., and Harden, C. S. Mass Spectrometry of Ion-Induced Water Clusters: An Explanation of the Infrared Continuum Absorption. Appl. Opt. *19*, 1776-1786 (1980).

4. Carlon, H. R. Limits of Detection for Condensation Nuclei Counters. J. Appl. Phys. *52*(4), 3062-3063 (1981).

5. Wilson, J. G. Principles of Cloud Chamber Technique. Cambridge University Press, London (1951).

6. Carlon, H. R. Variations in Emission Spectra from Warm Water Fogs: Evidence for Clusters in the Vapor Phase. Infrared Phys. *19*, 49-64.

7. Elsasser, W. M. Note on Atmospheric Absorption Caused by the Rotational Water Band. Phys. Rev. *53*, 768 (1938).

8. Varanasi. P. Chou, S., and Penner, S. S. Absorption Coefficients for Water Vapor in the 600-1000 cm^{-1} Region. J. Quant. Spectrosc. Radiat. Transfer *8*, 1537-1541 (1968).

DISTRIBUTION LIST 2

Names	Copies
CHEMICAL SYSTEMS LABORATORY	
ATTN: DRDAR-CLF	1
ATTN: DRDAR-CLC-B	1
ATTN: DRDAR-CLC-C	1
ATTN: DRDAR-CLC-E	1
ATTN: DRDAR-CLJ-R	2
ATTN: DRDAR-CLJ-L	2
ATTN: DRDAR-CLJ-M	1
ATTN: DRDAR-CLN	1
ATTN: DRDAR-CLW	1
ATTN: DRDAR-CLW-C	1
ATTN: DRDAR-CLW-P	1
ATTN: DRDAR-CLW-E	1
ATTN: DRDAR-CLB-C	1
ATTN: DRDAR-CLB-P	1
ATTN: DRDAR-CLB-PO	1
ATTN: DRDAR-CLB-R	1
ATTN: DRDAR-CLB-T	1
ATTN: DRDAR-CLB-TE	1
ATTN: DRDAR-CLY-A	1
ATTN: DRDAR-CLY-R	4
COPIES FOR AUTHOR(S): Research Division	1
RECORD SET: DRDAR-CLB-A	1
DEPARTMENT OF DEFENSE	
Defense Technical Information Center ATTN: DTIC-DDA-2 Cameron Station, Building 5 Alexandria, VA 22314	2
Director Defense Intelligence Agency ATTN: DB-4G1 Washington, DC 20301	1
Special Agent in Charge ARO, 902d Military Intelligence GP ATTN: IAGPA-A-AN Aberdeen Proving Ground, MD 21005	1
Commander SED, HQ, INSCOM ATTN: IRFM-SED (Mr. Joubert) Fort Meade, MD 20755	1
DEPARTMENT OF THE ARMY	
HQDA (DAMO-NCC) WASH DC 20310	1
HQDA, OCSA ATTN: DACS-FM, MG R. Anson Room 1A871, Pentagon Washington, Dc 20310	1
Federal Emergency Management Agency Office of Mitigation and Research ATTN: David W. Bensen Washington, DC 20472	1
Deputy Chief of Staff for Research, Development & Acquisition ATTN: DAMA-CSS-C ATTN: DAMA-ARZ-D Washington, DC 20310	1 1
Department of the Army Headquarters, Sixth US Army ATTN: AFKC-OP-NBC Presidio of San Francisco, CA 94129	1
US Army Research and Standardization Group (Europe) ATTN: DRXSN-E-SC Box 65, FPO New York 09510	1
HQDA (DAMI-FIT) WASH, DC 20310	1
Commander HQ 7th Medical Command ATTN: AEMPM APO New York 09403	1
Commander DARCOM, STITEUR ATTN: DRXST-STI Box 48, APO New York 09710	1
Commander US Army Science & Technology Center-Far East Office ATTN: MAJ Borges APO San Francisco 96328	1

Commander
2d Infantry Division
ATTN: EAIDCOM 1
APO San Francisco 96224

Commander
5th Infantry Division (Mech)
ATTN: Division Chemical Officer 1
Fort Polk, LA 71459

Commander
US Army Nuclear & Chemical Agency
ATTN: MONA-WE (LTC Pelletier) 1
7500 Backlick Rd, Bldg 2073
Springfield, VA 22150

Army Research Office
ATTN: DRXRO-CB 1
ATTN: DRXRO-MA 1
P.O. Box 12211
Research Triangle Park, NC 27709

OFFICE OF THE SURGEON GENERAL

Commander
US Army Medical Bioengineering
Research & Development Laboratory
ATTN: SGRD-UBD-AL 1
Fort Detrick, Bldg 568
Frederick, MD 21701

Headquarters
US Army Medical Research and
Development Command
ATTN: SGRD-PL 1
Fort Detrick, MD 21701

Commander
USA Medical Research Institute of
Chemical Defense
ATTN: SGRD-UV-L 1
Aberdeen Proving Ground, MD 21010

US ARMY HEALTH SERVICE COMMAND

Superintendent
Academy of Health Sciences
US Army
ATTN: HSA-CDH 1
ATTN: HSA-IPM 1
Fort Sam Houston, TX 78234

US ARMY MATERIEL DEVELOPMENT AND
READINESS COMMAND

Commander
US Army Materiel Development and
Readiness Command
ATTN: DRCLDC 1
ATTN: DRCSF-P 1
5001 Eisenhower Ave
Alexandria, VA 22333

Director
Human Engineering Laboratory
ATTN: DRXHE-SP (CB Defense Team) 1
Aberdeen Proving Ground, MD 21005

Commander
US Army Foreign Science & Technology
Center
ATTN: DRXST-MT3 1
220 Seventh St., NE
Charlottesville, VA 22901

Director
US Army Materiel Systems Analysis Activity
ATTN: DRXSY-MP 1
ATTN: DRXSY-CA (Mr. Metz) 2
Aberdeen Proving Ground, MD 21005

Commander
US Army Missile Command
Redstone Scientific Information Center
ATTN: DRSMI-RPR (Documents) 1
Redstone Arsenal, AL 35809

Director
DARCOM Field Safety Activity
ATTN: DRXOS-C 1
Charlestown, IN 47111

Commander
US Army Natick Research and
Development Command
ATTN: DRDNA-O 1
ATTN: DRDNA-VC 1
ATTN: DRDNA-VCC 1
ATTN: DRDNA-VM 1
ATTN: DRDNA-VR 1
ATTN: DRDNA-VT 1
Natick, MA 01760

US ARMY ARMAMENT RESEARCH AND DEVELOPMENT COMMAND

Commander
US Army Armament Research and Development Command
ATTN: DRDAR-LCA-L 1
ATTN: DRDAR-LCU-CE 1
ATTN: DRDAR-PMA (G.R. Sacco) 1
ATTN: DRDAR-SCA-W 1
ATTN: DRDAR-TSS 5
ATTN: DRCPM-CAWS-AM 1
ATTN: DRCPM-CAWS-SI 1
Dover, NJ 07801

US ARMY ARMAMENT MATERIEL READINESS COMMAND

Commander
US Army Armament Materiel Readiness Command
ATTN: DRSAR-ASN 1
ATTN: DRSAR-SF 1
ATTN: DRSAR-SR 1
Rock Island, IL 61299

Commander
USA ARRCOM
ATTN: SARTE 1
Aberdeen Proving Ground, MD 21010

Commander
US Army Dugway Proving Ground
ATTN: Technical Library (Docu Sect) 1
Dugway, UT 84022

US ARMY TRAINING & DOCTRINE COMMAND

Commandant
US Army Infantry School
ATTN: NBC Division 1
Fort Benning, GA 31905

Commandant
US Army Missile & Munitions Center and School
ATTN: ATSK-DT-MU-EOD 1
Redstone Arsenal, AL 35809

Commandant
USAMP&CS/TC&FM
ATTN: ATZN-CM-CDM 1
Fort McClellan, AL 36205

US Army Chemical School
ATTN: ATZN-CM-AL 1
Fort McClellan, AL 36205

Commander
US Army Infantry Center
ATTN: ATSH-CD-MS-C 1
Fort Benning, GA 31905

Commander
US Army Infantry Center
Directorate of Plans & Training
ATTN: ATZB-DPT-PO-NBC 1
Fort Benning, GA 31905

Commander
USA Training and Doctrine Command
ATTN: ATCD-Z 1
Fort Monroe, VA 23651

Commander
USA Combined Arms Center and Fort Leavenworth
ATTN: ATZL-CA-COG 1
ATTN: ATZL-CAM-IM 1
Fort Leavenworth, KS 66027

Commander
US Army TRADOC System Analysis Activity
ATTN: ATAA-SL 1
White Sands Missile Range, NM 88002

US ARMY TEST & EVALUATION COMMAND

Commander
US Army Test & Evaluation Command
ATTN: DRSTE-CT-T 1
Aberdeen Proving Ground, MD 21005

DEPARTMENT OF THE NAVY

Chief of Naval Research
ATTN: Code 443 1
800 N. Quincy Street
Arlington, VA 22217

Commander
Naval Explosive Ordnance Disposal Facility
ATTN: Army Chemical Officer (Code AC-3) 1
Indian Head, MD 20640

Commander
Naval Surface Weapons Center
Code G51 1
Dahlgren, VA 22448

Chief, Bureau of Medicine & Surgery
Department of the Navy
ATTN: MED 3C33 1
Washington, DC 20372

Commander
Naval Weapons Center
ATTN: Technical Library (Code 343) 1
China Lake, CA 93555

US MARINE CORPS

Director, Development Center
Marine Corps Development and
Education Command
ATTN: Fire Power Division 1
Quantico, VA 22134

DEPARTMENT OF THE AIR FORCE

HQ Foreign Technology Division (AFSC)
ATTN: TQTR 1
Wright-Patterson AFB, OH 45433

Commander
Aeronautical Systems Division
ATTN: ASD/AESD 1
Wright-Patterson AFB, OH 45433

HQ AFLC/LOWMM 1
Wright-Patterson AFB, OH 45433

HQ, AFSC/SDNE 1
Andrews AFB, MD 20334

HQ AMD/RD
ATTN: Chemical Defense OPR 1
Brooks AFB, TX 78235

NORAD Combat Operations Center
ATTN: DOUN 1
Cheyenne Mtn Complex, CO 80914

AFAMRL/HE
ATTN: Dr. Clyde Replogle 1
Wright-Patterson AFB, OH 45433

HQ AFTEC/SGB 1
Kirtland AFB, NM 87117

USAF TAWC/THLO 1
Eglin AFB, FL 32542

USAFSAM/HR
ATTN: Dr. Robert Reyes 1
Brooks AFB, TX 78235

USAFSAM/VNT
ATTN: Dr. F. Wesley Baumgardner 1
Brooks AFB, TX 78235

AFAMRL/HE
ATTN: COL Dan Johnson 1
Wright-Patterson AFB, OH 45433

AMD/RDE
ATTN: LTC T. Kingery 1
Brooks AFB, TX 78235

OUTSIDE AGENCIES

Battelle, Columbus Laboratories
ATTN: TACTEC 1
505 King Avenue
Columbus, OH 43201

Toxicology Information Center, WG 1008
National Research Council 1
2101 Constitution Ave., NW
Washington, DC 20418

US Public Health Service
Center for Disease Control
ATTN: Lewis Webb, Jr. 1
Building 4, Room 232
Atlanta, GA 30333